Angewandte Chemie
Eine Zeitschrift der Gesellschaft Deutscher Chemiker

Supporting Information

69451 Weinheim, Germany

Snapshots of the Reaction Mechanism of Matrix Metalloproteinases

Ivano Bertini,[*,1,2] Vito Calderone,[1] Marco Fragai, [1,3] Claudio Luchinat,[1,3] Massimiliano Maletta,[1,2] Kwon Joo Yeo[1]

[1] Magnetic Resonance Center (CERM) – University of Florence, Via L. Sacconi 6, 50019 Sesto Fiorentino, Italy

[2] Department of Chemistry – University of Florence, Via della Lastruccia 3, 50019 Sesto Fiorentino, Italy

[3] Department of Agricultural Biotechnology, University of Florence, Via Maragliano, 75-77, 50144 Florence, Italy.

[*]**Prof. Ivano Bertini**
Magnetic Resonance Center (CERM)
University of Florence
Via L. Sacconi 6
50019 Sesto Fiorentino, Italy
e-mail: ivanobertini@cerm.unifi.it
Tel.: +390554574272
Fax: +390554574271

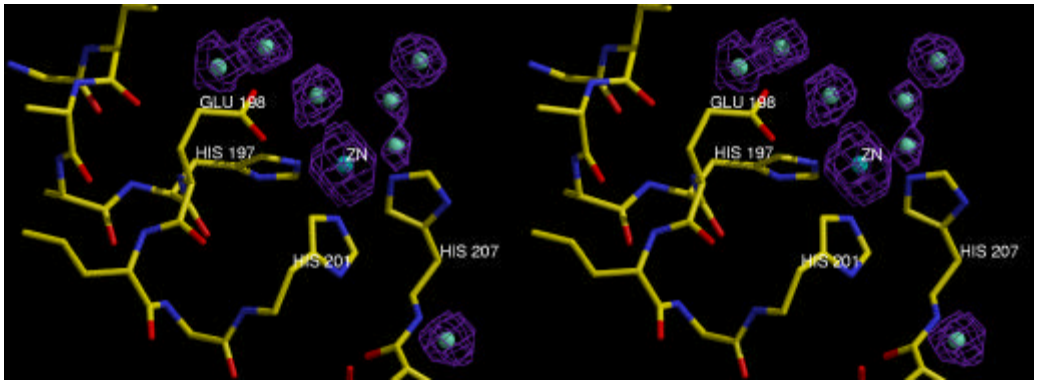

A

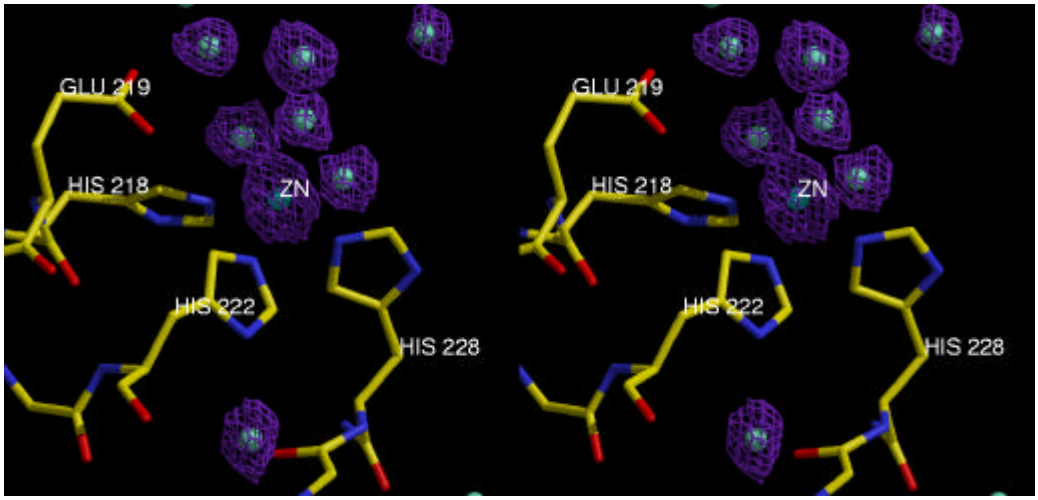

B

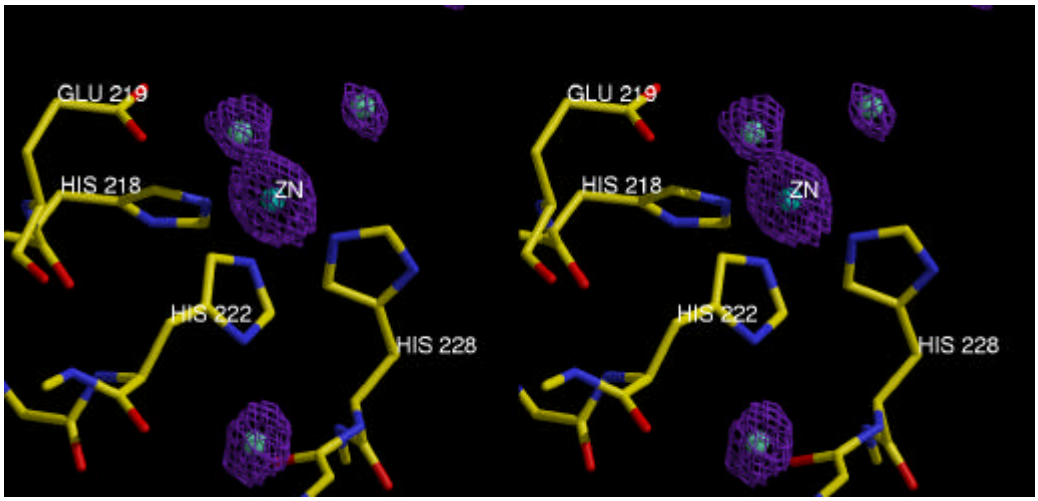

C

Figure S1. 2Fo-Fc electron density map contoured at 1σ level showing zinc and its coordinated water molecules in **A**) Active MMP-8, **B**) Active MMP-12 and **C**) One peptide MMP-12 adduct.

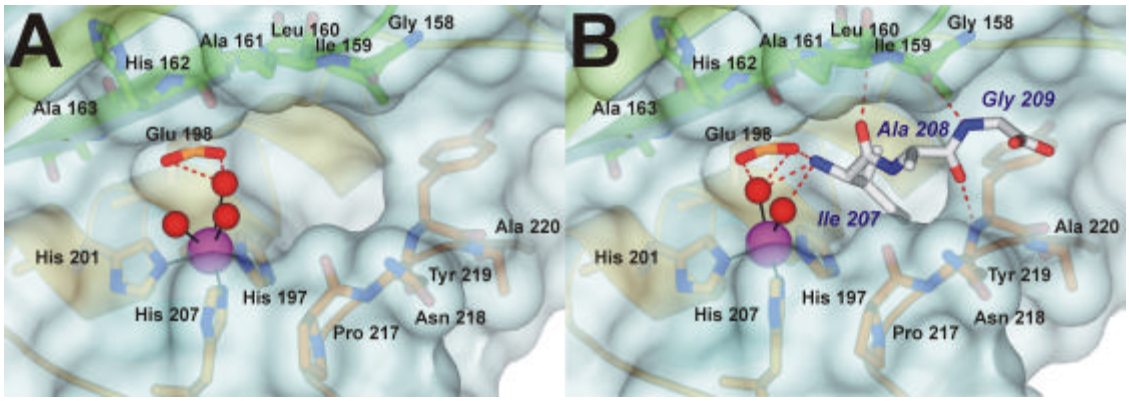

Figure S2. Active, uninhibited form of MMP-8 (A) and its *IleAlaGly* adduct (B).

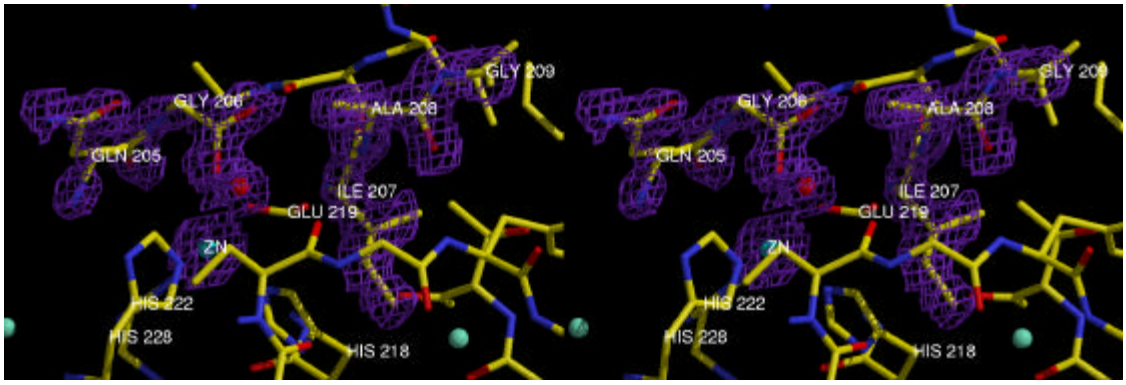

A

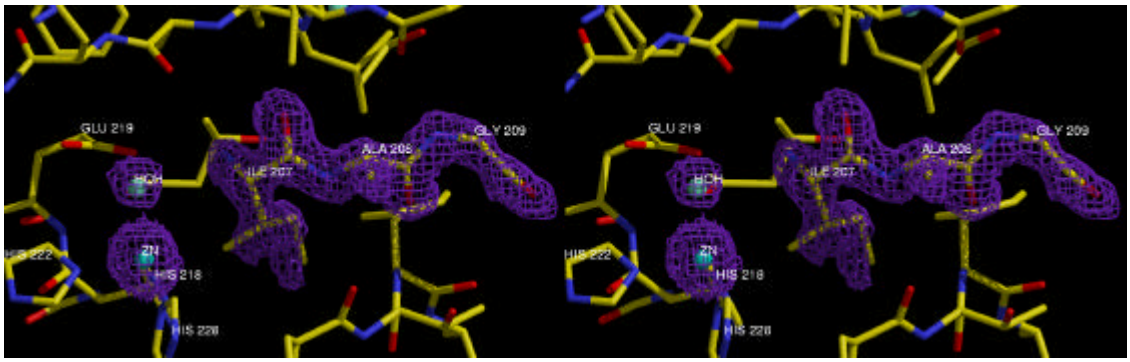

B

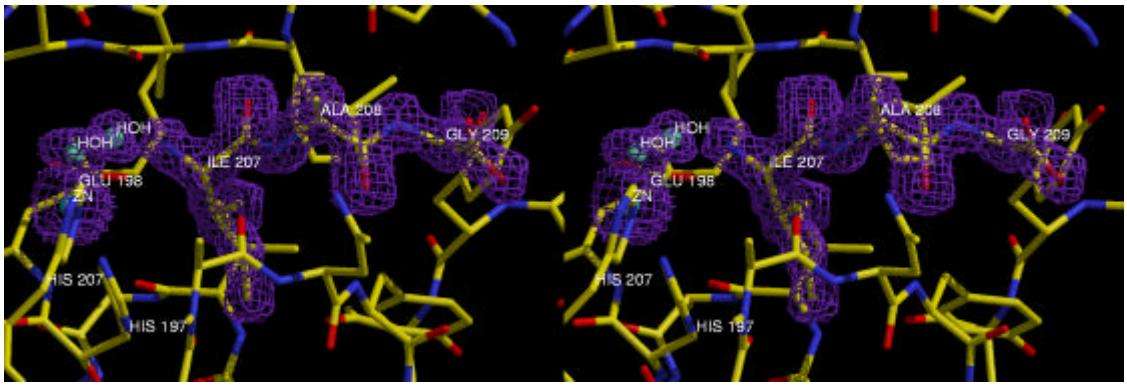

C

Figure S3. 2Fo-Fc electron density map contoured at 1σ level showing zinc and its coordinated water molecules and the bound peptide(s) in **A**) Two-peptide MMP-12 adduct, **B**) One peptide MMP-12 adduct and **C**) One peptide MMP-8 adduct.

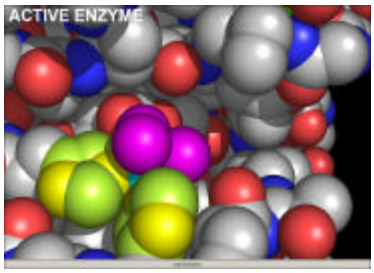

(set the player *repeat* option on)

Movie S1. A four-frame movie of 1) active MMP, 2) its modelled gem-diol intermediate with the central part of the *ProGlnGlyIleAlaGly* peptide; 3) the two-peptide intermediate; 4) the one-peptide intermediate. The movie is based on the MMP-12 structures, where the gem-diol intermediate[29] in frame (B) is modelled after the uninhibited (Figure 1A) and two-peptide (Figure 1C) forms. Atom colors are CPK except zinc (cyan), its histidine ligands (yellow = N, limon = C), and coordinated water molecules (magenta). Hydrogens are not shown.

Crystallization, Data Collection and Structure Solution

Crystals of human MMP-12 were obtained as previously reported.[1] Crystals of human MMP-8 grew using the same technique at 20° C from a solution containing 0.1 M Tris-HCl, 20% PEG-3350, 200 mM AHA, 0.2 M $MgCl_2$ at pH 8.0. The final protein concentration was 0.4 mM. The crystallization buffer contained 200 mM of the weak inhibitor acetohydroxamic acid (AHA). To obtain the active uninhibited enzymes, MMP crystals were then extensively dialyzed against the same crystallization buffers lacking AHA. The *ProGlnGlyIleAlaGly* peptide (INBIOS s.r.l., Naples) was soaked into the crystals for 1-3 days in order to obtain the two- or the one-peptide adducts.

The peptide was added, in powder form, directly into the drop using a needle and was left incubating for 1-3 days. MMP-12 two-peptide complex (A) was measured in-house, using a PX-Ultra copper sealed tube source (Oxford Diffraction) equipped with an Onyx CCD detector, whereas the single-peptide complex (B) was measured using synchrotron radiation at ID-29 beamline (ESRF, Grenoble, France). Active MMP-12 (C) and the MMP-8 one-peptide complex (D) were measured at beamline BW7B (DESY, Hamburg, Germany), whereas active MMP-8 (E) was measured at beamline ID23-1 (ESRF, Grenoble, France). All datasets were collected at 100 K and the crystals used for data collection were cryo-cooled without any cryo-protectant treatment.

A diffracted to 1.9 Å resolution, B diffracted to 1.2 Å and C to 1.3 Å; they all belong to spacegroup C2 with one molecule in the asymmetric unit, a solvent content of about 50% and a mosaicity of 0.7°-0.8°. D diffracted to 1.5 Å resolution in space group $P2_1$ with two molecules in the asymmetric unit whereas E diffracted to 1.7 Å resolution in space group P1 with two molecules in the asymmetric unit. Solvent content and mosaicity values for D and E are roughly 50% and 0.8°-0.9° respectively.

The data were processed in all cases using the program MOSFLM[2] and scaled using the program SCALA[3] with the TAILS and SECONDARY corrections on (the latter restrained with a TIE SURFACE command) to achieve an empirical absorption correction. Table 1 shows the data collection and processing statistics for all datasets. The structures were solved using the molecular replacement technique; the model used for all MMP-12 datasets was 1Y93 whereas the one used for MMP-8 datasets was 1I73; in all

cases inhibitors, water molecules and ions were omitted from the models. The correct orientation and translation of the molecule within the crystallographic unit cell was determined with standard Patterson search techniques[4,5] (as implemented in the program MOLREP.[6;7] The isotropic refinement was carried out using REFMAC5[8] on A and E datasets but metal ion B-factors were refined taking anisotropy into account; conversely, datasets B, C and D were refined taking anisotropy into account for all atoms. REFMAC5 default weights for the crystallographic term and the geometrical term have been used in all cases.

In between the refinement cycles the models were subjected to manual rebuilding by using XtalView.[9] The same program was used to model ligands. Water molecules have been added by using the standard procedures within the ARP/WARP suite.[10] The stereochemical quality of the refined models was assessed using the program Procheck.[11] The Ramachandran plot is in all cases of very good quality.

Table 1 reports the data collection and refinement statistics for all datasets.

Modelling of the gem-diol

The gem-diol adduct of MMP-12 was modeled using the experimental structures of the active enzyme (Figure 1A) and of the two-peptide adduct (Figure 1C) as the starting point and the gem-diol coordination geometry experimentally observed for a transition state analog.[29]

The model was refined using the *local search* option of Autodock.[12] The standard, validated Autodock zinc parameters for MMP were used.[13;14] A final minimization of both models using Amber[15] converged to the single structure of Figure 1B.

	His218	His222	His228	HOH1 (Glu219)	HOH2	HOH3
Active MMP-12	2.13	2.12	2.09	2.40	2.38	2.10
Two-peptide MMP-12	2.11	2.00	2.02	2.83	2.37	-
One-peptide MMP-12	2.04	2.08	2.04	2.28	-	-
Active MMP-8 (two molecules)	2.06 2.09	2.22 2.06	2.14 2.20	2.84 2.69	2.70 -	2.79 -
One-peptide MMP-8 (two molecules)	2.07 2.06	2.10 2.12	2.04 2.00	2.27 2.19	2.35 2.48	- -

Table S1. Distances between Zn and the three coordinated histidines, between the Glu-activated water molecules and zinc and between Zn and the other water molecules coordinated to it.

Table S2.

Table 1.	**DATA COLLECTION AND REFINEMENT STATISTICS**				
	Two-peptide-MMP12 complex (A)	Active MMP-12 (C)	One-peptide-MMP12 complex (B)	Active MMP-8 (E)	One-peptide-MMP8 complex (D)
Spacegroup	C2	C2	C2	P1	$P2_1$
Cell dimensions (Å, °)	a= 51.54 b= 60.37 c= 54.45 β= 115.41	a= 51.54 b= 60.75 c= 54.26 β= 115.64	a= 51.89 b= 60.36 c= 54.52 β= 115.73	a= 33.29 b= 47.11 c= 61.32 α= 77.73 β= 80.03 γ= 77.01	a= 33.21 b= 68.53 c= 78.28 β= 98.10
Resolution (Å)	30.2 – 1.9	25.8 – 1.2	49.0 – 1.1	39.5 – 1.7	38.7 – 1.5
Unique reflections	11726 (1505)	41969 (5315)	50850 (7153)	30329 (4603)	55607 (8108)
Overall completeness (%)	98.1 (86.9)	97.2 (84.8)	94.6 (91.1)	90.3 (88.3)	99.9 (99.9)
R_{sym} (%)	13.7 (32.7)	7.9 (12.6)	5.9 (15.6)	10.3 (24.5)	8.2 (31.4)
Multiplicity	5.6 (3.0)	5.8 (5.2)	6.8 (6.8)	1.5 (1.5)	6.7 (6.0)
I/(σI)	4.7 (2.3)	5.1 (3.8)	4.2 (4.1)	4.7 (2.6)	6.6 (2.2)
Wilson plot B-factor ($Å^2$)	7.69	7.17	11.08	16.14	10.21
R_{cryst} / R_{free} (%)	20.6 / 28.7	19.6 / 21.6	19.7 / 22.2	22.5 / 29.3	16.3 / 19.2
Protein atoms	1238	1238	1238	2480 (two molecules)	2480 (two molecules)
Ions	5	5	5	8	8
Ligand atoms	31	0	17	0	17
Water molecules	119	238	206	303	591
RMSD bond lengths (Å)	0.021	0.007	0.007	0.020	0.008
RMSD bond angles (°)	1.8	1.0	1.1	1.6	1.1
Mean B-factor ($Å^2$)	9.80	11.00	14.16	17.17	12.39

PROCHECK

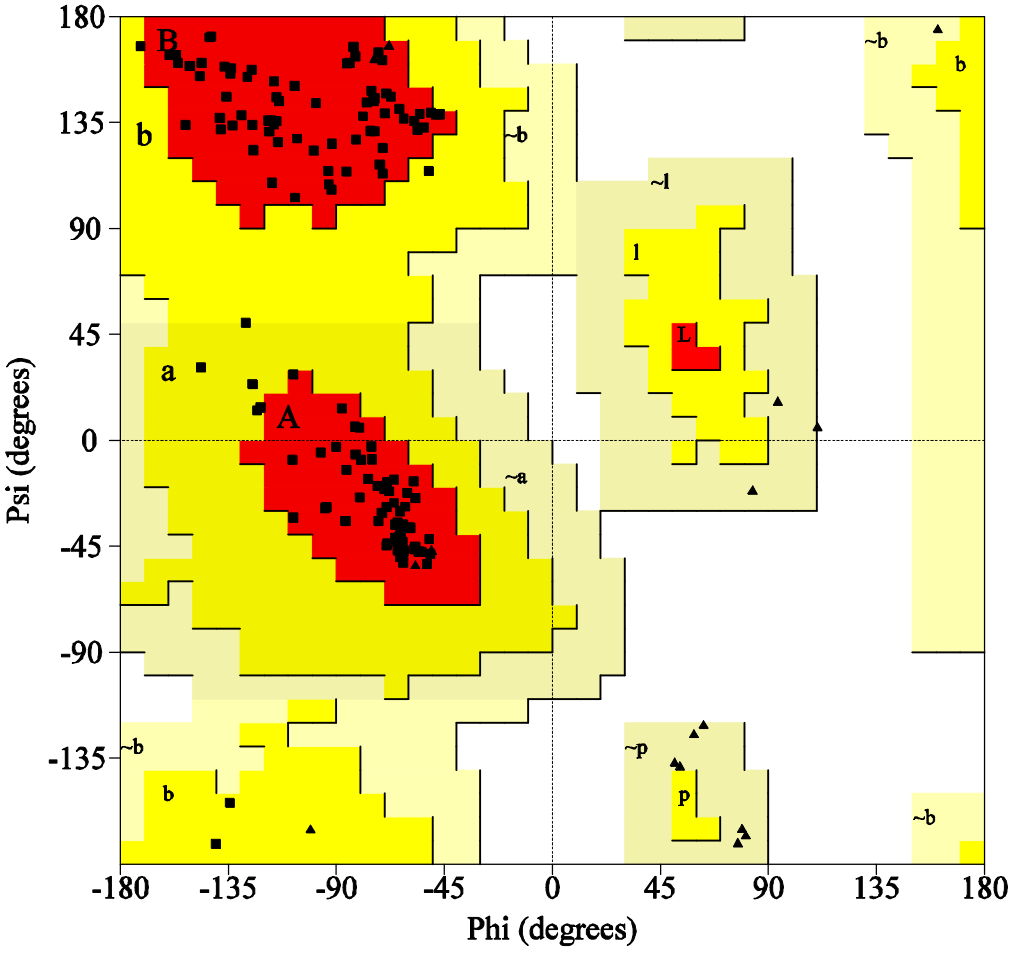

Plot statistics

Residues in most favoured regions [A,B,L]	124	93.2%
Residues in additional allowed regions [a,b,l,p]	9	6.8%
Residues in generously allowed regions [~a,~b,~l,~p]	0	0.0%
Residues in disallowed regions	0	0.0%
Number of non-glycine and non-proline residues	133	100.0%
Number of end-residues (excl. Gly and Pro)	240	
Number of glycine residues (shown as triangles)	19	
Number of proline residues	6	
Total number of residues	398	

Based on an analysis of 118 structures of resolution of at least 2.0 Angstroms and R-factor no greater than 20%, a good quality model would be expected to have over 90% in the most favoured regions.

A

PROCHECK

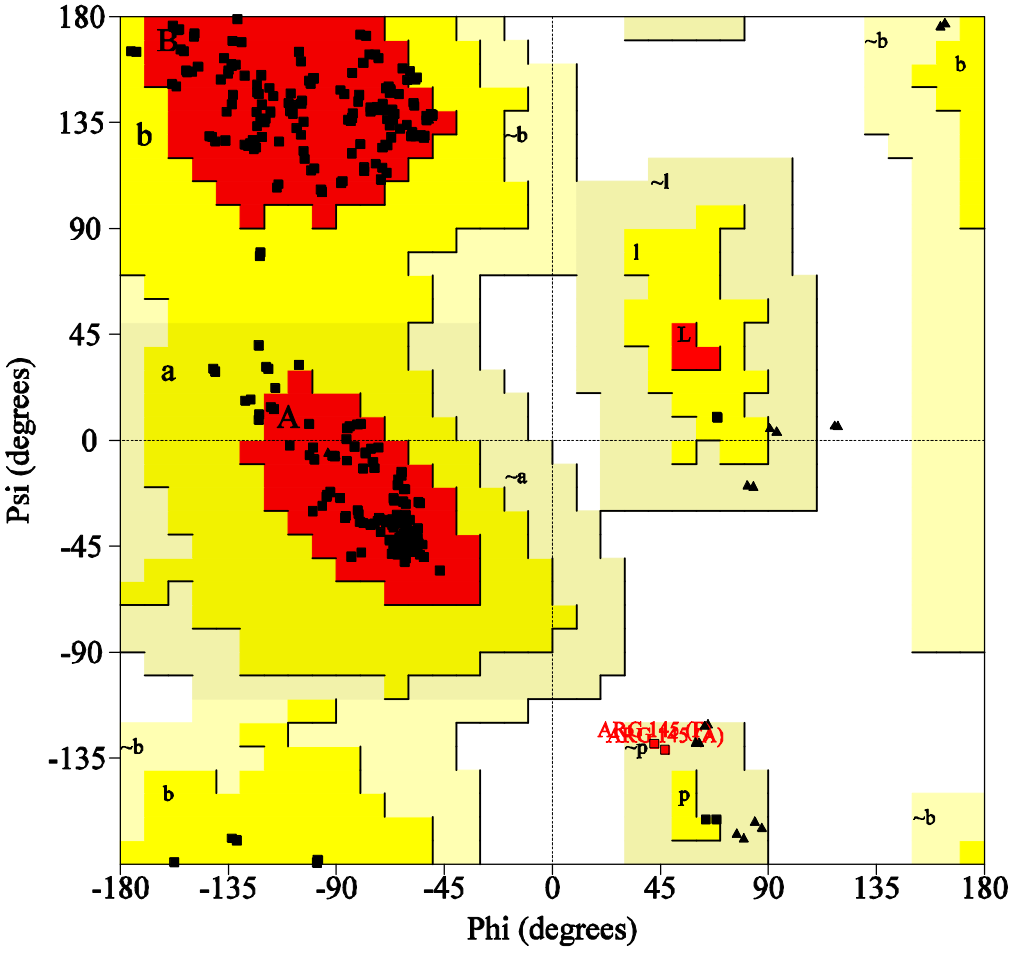

Plot statistics

Residues in most favoured regions [A,B,L]	245	90.1%
Residues in additional allowed regions [a,b,l,p]	25	9.2%
Residues in generously allowed regions [~a,~b,~l,~p]	2	0.7%
Residues in disallowed regions	0	0.0%
Number of non-glycine and non-proline residues	272	100.0%
Number of end-residues (excl. Gly and Pro)	575	
Number of glycine residues (shown as triangles)	28	
Number of proline residues	18	
Total number of residues	893	

Based on an analysis of 118 structures of resolution of at least 2.0 Angstroms and R-factor no greater than 20%, a good quality model would be expected to have over 90% in the most favoured regions.

B

PROCHECK

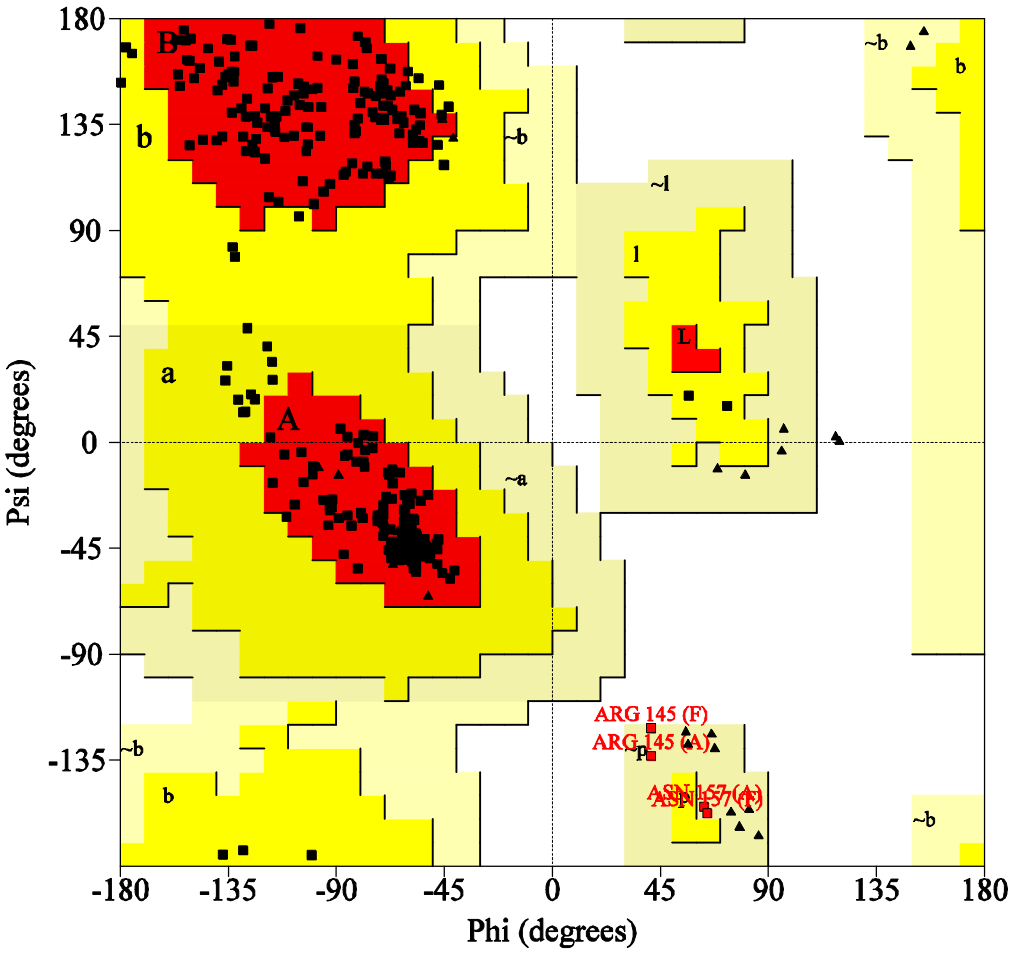

Plot statistics

Residues in most favoured regions [A,B,L]	241	89.3%
Residues in additional allowed regions [a,b,l,p]	25	9.3%
Residues in generously allowed regions [~a,~b,~l,~p]	4	1.5%
Residues in disallowed regions	0	0.0%
Number of non-glycine and non-proline residues	270	100.0%
Number of end-residues (excl. Gly and Pro)	304	
Number of glycine residues (shown as triangles)	26	
Number of proline residues	18	
Total number of residues	618	

Based on an analysis of 118 structures of resolution of at least 2.0 Angstroms and R-factor no greater than 20%, a good quality model would be expected to have over 90% in the most favoured regions.

C

PROCHECK

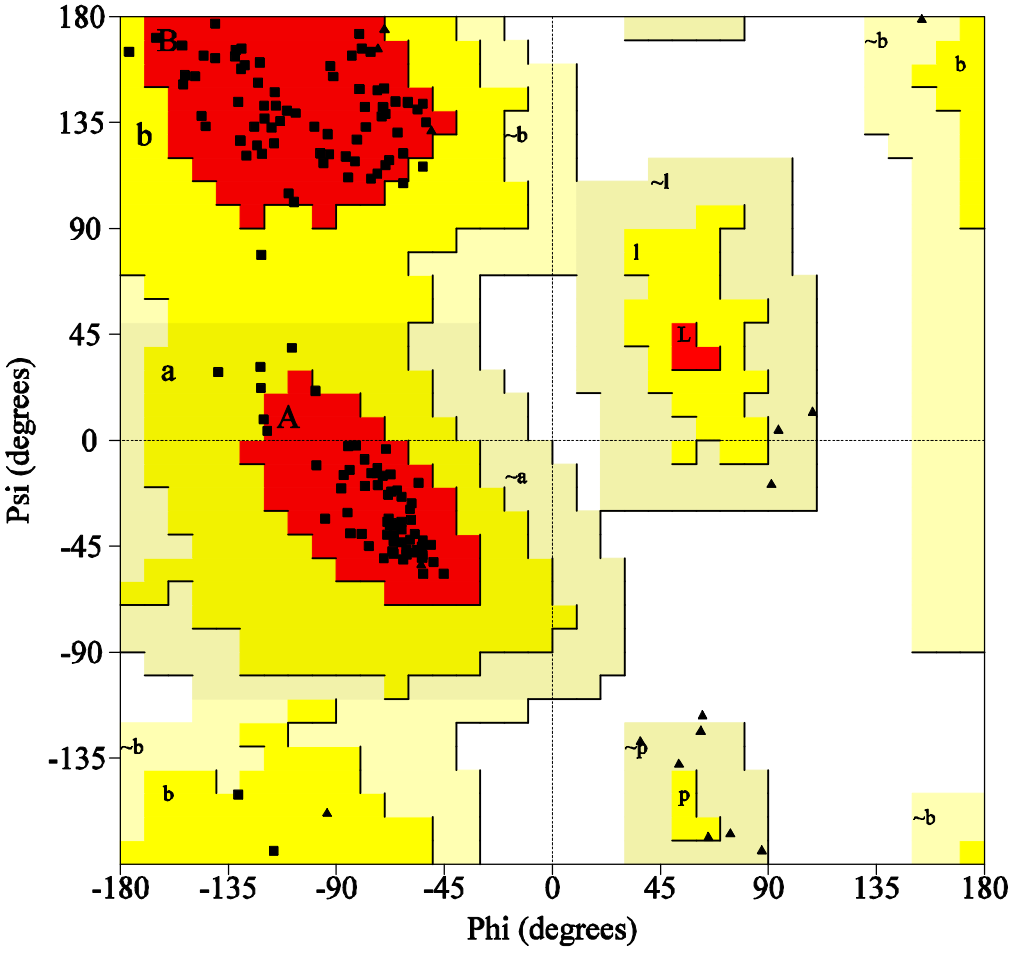

Plot statistics

Residues in most favoured regions [A,B,L]	122	91.0%
Residues in additional allowed regions [a,b,l,p]	12	9.0%
Residues in generously allowed regions [~a,~b,~l,~p]	0	0.0%
Residues in disallowed regions	0	0.0%
Number of non-glycine and non-proline residues	134	100.0%
Number of end-residues (excl. Gly and Pro)	115	
Number of glycine residues (shown as triangles)	21	
Number of proline residues	6	
Total number of residues	276	

Based on an analysis of 118 structures of resolution of at least 2.0 Angstroms and R-factor no greater than 20%, a good quality model would be expected to have over 90% in the most favoured regions.

D

PROCHECK

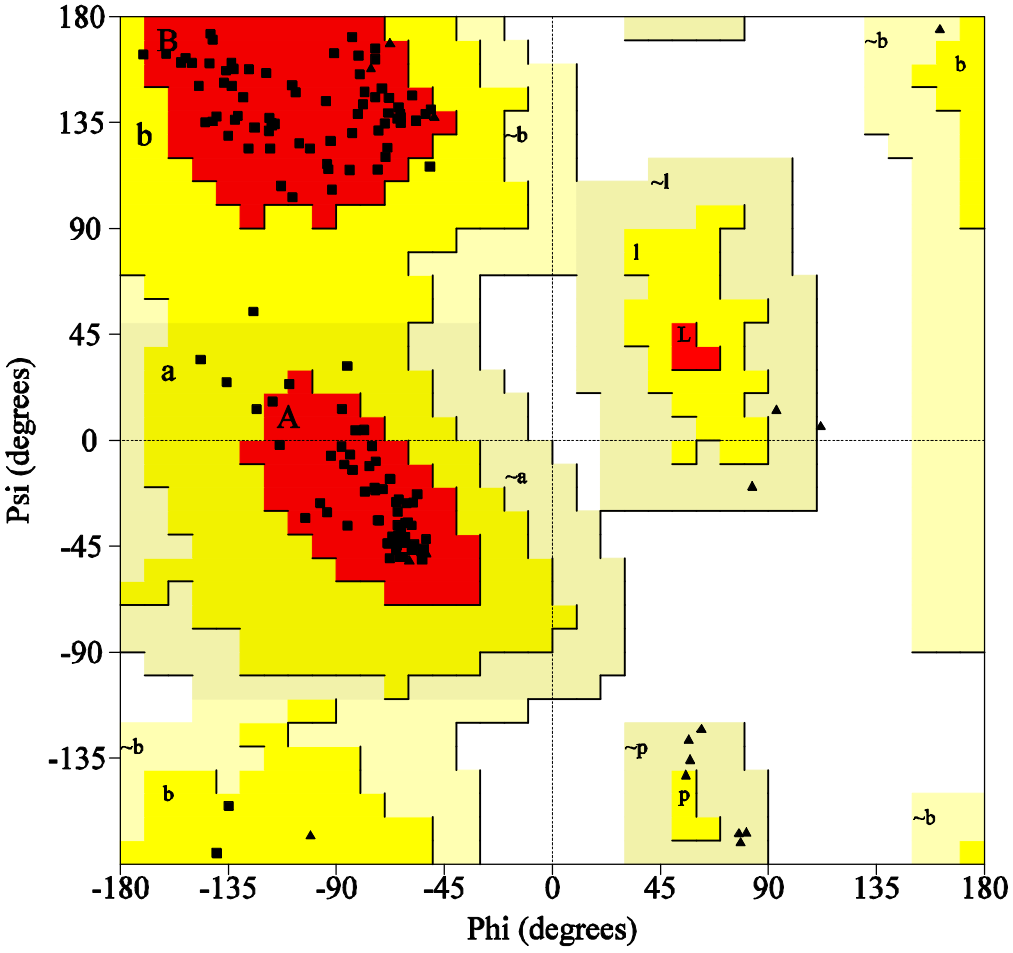

Plot statistics

Residues in most favoured regions [A,B,L]	126	94.0%
Residues in additional allowed regions [a,b,l,p]	8	6.0%
Residues in generously allowed regions [~a,~b,~l,~p]	0	0.0%
Residues in disallowed regions	0	0.0%
Number of non-glycine and non-proline residues	134	100.0%
Number of end-residues (excl. Gly and Pro)	205	
Number of glycine residues (shown as triangles)	20	
Number of proline residues	6	
Total number of residues	365	

Based on an analysis of 118 structures of resolution of at least 2.0 Angstroms and R-factor no greater than 20%, a good quality model would be expected to have over 90% in the most favoured regions.

E

Figure S4. Ramachandran plots for A) Active MMP-12, B) One peptide MMP-8 adduct, C) Active MMP-8, D) Two peptide MMP-12 adduct and E) One peptide MMP-12 adduct.

References

[1] I. Bertini, V. Calderone, M. Cosenza, M. Fragai, Y.-M. Lee, C. Luchinat, S. Mangani, B. Terni, P. Turano, *Proc. Natl. Acad. Sci. USA* **2005**, *102*, 5334-5339.

[2] A. G. W. Leslie, in *Molecular data processing*Eds.: D. Moras, A. D. Podjarny, J.-C. Thierry, Oxford University Press, Oxford **1991**, 50-61.

[3] P. R. Evans, "Data Reduction", Proceedings of CCP4 Study Weekend, *"Data Reduction", Proceedings of CCP4 Study Weekend*, pp. 114-122 .

[4] M. G. Rossmann, D. M. Blow, *Acta Cryst.* **1962,** *D15*, 24-31.

[5] R. A. Crowther, Ed.: M. G. Rossmann), Gordon & Breach, New York **1972**.

[6] A. Vagin, A. Teplyakov, *J.Appl.Crystallogr.* **1997,** *30*, 1022-1025.

[7] A. Vagin, A. Teplyakov, *Acta Crystallogr D Biol Crystallogr* **2000,** *56*, 1622-1624.

[8] G. N. Murshudov, A. A. Vagin, E. J. Dodson, *Acta Cryst.* **1997,** *D53*, 240-255.

[9] D. E. McRee, *J.Mol.Graphics* **1992,** *10*, 44-47.

[10] V. S. Lamzin, *Acta Crystallogr D Biol Crystallogr* **1993,** *49*, 129-147.

[11] R. A. Laskowski, M. W. MacArthur, D. S. Moss, J. M. Thornton, *J.Appl.Crystallogr.* **1993,** *26*, 283-291.

[12] G. M. Morris, D. S. Goodsell, R. S. Halliday, R. Huey, W. E. Hart, R. K. Belew, A. J. Olson, *J Comp Chem* **1998,** *19*, 1639-1662.

[13] X. Hu, W. H. Shelver, *J.Mol.Graph.Model.* **2003,** *22*, 115-126.

[14] I. Bertini, M. Fragai, A. Giachetti, C. Luchinat, M. Maletta, G. Parigi, K. J. Yeo, *J.Med.Chem.* **2005,** *48*, 7544-7559.

[15] Case, D. A., Darden, T. A., Cheatham, T. E., Simmerling, C. L., Wang, J., et. al. AMBER 8, 2004. San Francisco, CA, University of California.